



A comparison study of polymer/cobalt ferrite nano-composites synthesized by mechanical alloying route

Sedigheh Rashidi, and Abolghasem Ataie *

School of Metallurgy and Materials Engineering, College of Engineering, University of Tehran, P.O. Box 14395-553, Tehran, Iran

Received: September 15, 2015; Accepted: November 29, 2015

* Corresponding author E-mail: ataaie@ut.ac.ir, Tel.: +98 21 82084084; Fax: +98 21 8800 6076

Abstract

In this research, the effect of different biopolymers such as polyethylene glycol (PEG) and polyvinyl alcohol (PVA) on synthesis and characterization of polymer/cobalt ferrite (CF) nano-composites by mechanical alloying method has been systematically investigated. The structural, morphological and magnetic properties changes during mechanical milling were investigated by X-ray diffraction (XRD), Fourier transform infrared spectroscopy (FTIR), transmission electron microscopy (TEM), field emission scanning electron microscopy (FESEM), and vibrating sample magnetometer techniques (VSM), respectively. The polymeric cobalt ferrite nano-composites were obtained by employing a two-step procedure: the cobalt ferrite of 20 nm mean particle size was first synthesized by mechanical alloying route and then was embedded in PEG or PVA biopolymer matrix by milling process. The results revealed that PEG melted due to the local temperature raise during milling. Despite this phenomenon, cobalt ferrite nano-particles were entirely embedded in PEG matrix. It seems, PAV is an appropriate candidate for producing nano-composite samples due to its high melting point. In PVA/CF nano-composites, the mean crystallite size and milling induced strain decreased to 13 nm and 0.48, respectively. Moreover, milling process resulted in well distribution of CF in PVA matrix even though the mean particle size of cobalt ferrite has not been significantly affected. FTIR result confirmed the attachment of PVA to the surface of nano-particles. Magnetic properties evaluation showed that saturation magnetization and coercivity values decreased in nano-composite sample comparing the pure cobalt ferrite.

Keywords: *cobalt ferrite nano-particles, mechanical alloying, nano-composite, polyvinyl alcohol, polyethylene glycol.*

1. Introduction

Organic-inorganic nano-composites, due to their remarkable chemical and physical

properties, that inherent from both components, have attracted considerable

attention in the past few years [1, 2]. Particularly, polymer/magnetic ferrite nano-composites have been an extremely active field of research because of their significant potential applications in various fields, ranging from technology to biomedicine, like magnetic resonance imaging (MRI), targeted drug delivery and hyperthermia [3].

Among the many magnetic nano-particles, cobalt ferrite (CoFe_2O_4) is an important spinel ferrite due to its relatively high coercivity, reasonable saturation magnetization, high surface area and mechanical hardness. It has been widely used in high density recording media, magnetic fluid, and biomedical field [4].

Embedding magnetic cobalt ferrite nano-particles in polymer matrix prevents their agglomeration, improves their chemical stability and biocompatibility. Hence, two biopolymers were selected, including polyethylene glycol (PEG) and polyvinyl alcohol (PVA), for the incorporation of cobalt ferrite nano-particles. Selection of PEG or PVA polymer was based on the following reasons: their biocompatibility, nontoxicity, water solubility, low cost, non-inflammability and multiple uses in different industrial-commercial segments [5, 6].

Up to present, several methods, such as sol-gel [6], co-precipitation [5], mini-emulsion polymerization [7] and microwave synthesis [8] have been developed in order to synthesize polymeric magnetic nano-composites. These methods, however, have difficulties, including high temperature synthesis, high cost and preparation of complex solution [9]. Consequently, mechanical alloying method was employed as an alternative way to overcome these difficulties.

Mechanical alloying is a powerful technique for the preparation of various types of oxide compounds, as well as novel functional nano-

sized materials. It has been shown that enhanced reaction rate can be achieved and dynamically maintained during milling as result of microstructural refinement and mixing process, accompanying repeated fracture, welding and deformation of particles during collision events [10]. For the first time, Shaw et al. [11] reported that mechanical milling could be applied for polymers. While there are some works in the synthesis of different polymer/magnetic metal composites by mechanical milling [12-14], little attention has been given to the preparation of polymer/magnetic ferrite nano-composites [15, 16].

To the best of our knowledge, there is no attempt on the synthesis of polymer/cobalt ferrite nano-composites by this method until now. Hence, in the present work mechanical alloying as a facile, low cost and solvent free method is applied for synthesis of polymer/ CoFe_2O_4 nano-composites and the effects of polymer type and milling time on the characteristics of nano-composites were investigated in details.

2. Experimental procedure

Cobalt ferrite nano-particles powder was synthesized via mechanical alloying route. The details of synthesis procedure were mentioned in our earlier work [17]. To prepare polymeric magnetic nano-composites, the synthesized cobalt ferrite nano-particles were mixed with 50 wt. % of PVA or PEG. The characteristics of the polymers are summarized in Table 1. The powder mixtures were milled using a planetary ball mill PM2400 with hardened chrome steel vial and 15 mm diameter grinding balls under air atmosphere. Milling was carried out for different milling times at two rotation speeds and ball to powder weight ratios (BPR). To avoid excessive heating, milling was interrupted frequently, twice an hour, for 10 minutes. The details of milling conditions are also listed in Table 2.

Table 1. Specifications of polymers used in this research

Polymer	Chemical formula	Density (g/cm^3)	Melting point ($^{\circ}\text{C}$)	Purity (%)	Company
PVA (72000)	$(\text{C}_2\text{H}_4\text{O})_n$	1.29	230	<99.0	Merck
PEG (6000)	$\text{C}_{2n}\text{H}_{4n+2}\text{O}_{n+1}$	1.21	54-58	Commercial	—

Table 2. Milling conditions of the nano-composite samples

Sample identity	Rotation speed (rpm)	BPR	Milling time (h)
PEG/CF1	300	15: 1	5
PEG/CF2	200	10: 1	10
PVA/CF	300	15: 1	10

The phase composition of the samples were studied by X-ray diffraction (XRD) at room temperature, using a Philips PW-3710 diffract meter with Cu- $K\alpha$ radiation ($\lambda=0.15406$ nm). The mean crystallite size and the internal strain of the milled powders were estimated using Williamson-Hall plot [18]. Morphology of cobalt ferrite nano-particles, together with its corresponding nano-composites were determined by using a high-resolution transmission electron microscope (HRTEM, JEOL, JEM-2100, operating at 200 kV) and field emission scanning electron microscope (FESEM, Hitachi S4160), respectively. The interaction between magnetic nano-particles

and polymer chains was confirmed by Fourier transform infrared spectroscopy (FTIR, Bruker), in the range of 400 to 4000 cm^{-1} . Magnetic properties of the samples were also measured using vibrating sample magnetometer (VSM) under a maximum magnetic field of 10 kOe.

3. Results and Discussion

The XRD pattern and TEM image of pure cobalt ferrite nano-particles, after 25 h milling are shown in Figure 1. As it is seen expected of the CoFe_2O_4 phase, no additional compositions were detected; indicating a single-phase crystalline spinel cobalt ferrite structure. The mean crystallite size of cobalt ferrite, using William-son Hall plot was found to be 15 nm. Typical bright field TEM image with its corresponding selected areas diffraction (SAD) pattern of cobalt ferrite in Figure 1 (b and c) illustrates the agglomerated nano-particles with a mean particle size of 20,

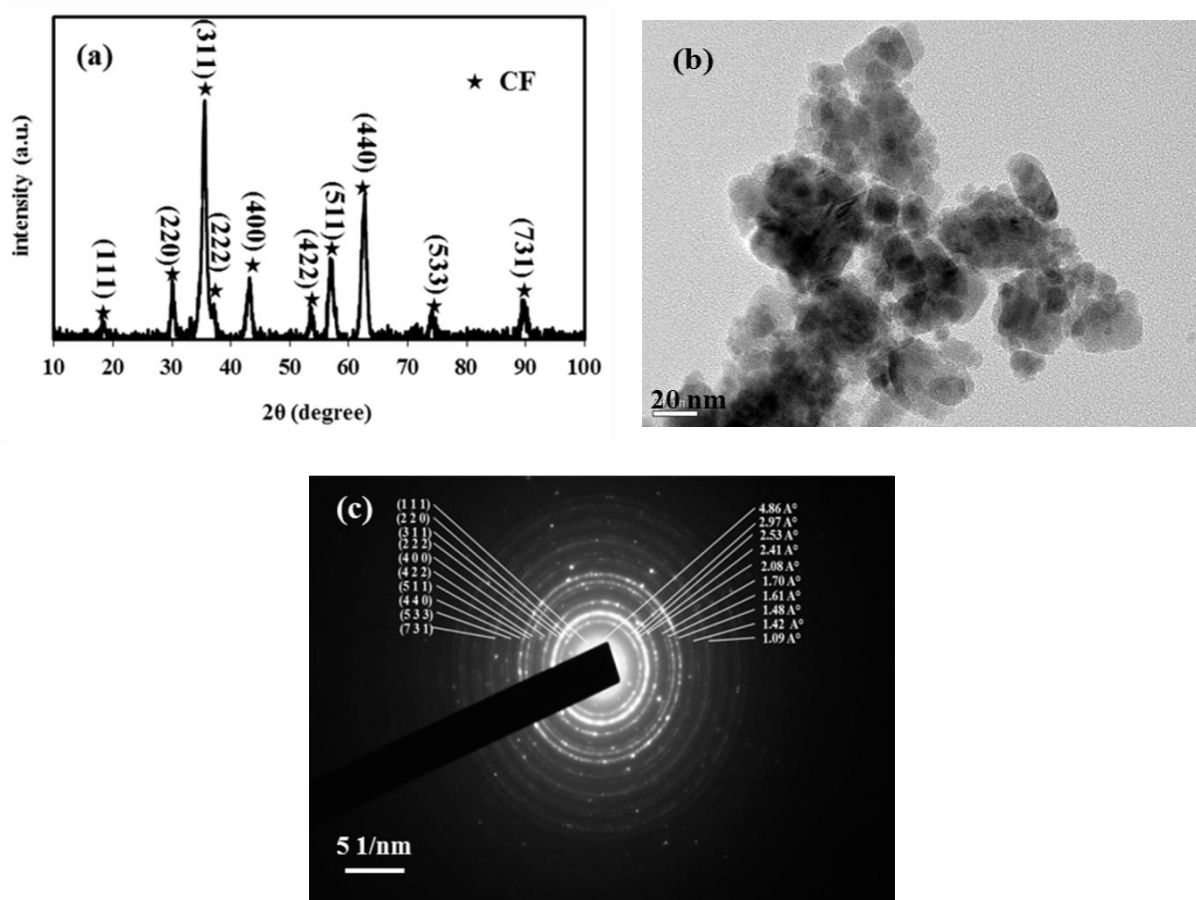


Fig. 1. XRD pattern (a), TEM image (b) and SAD pattern (c) of pure CF nano-particles

with mainly a spherical shape. The dipole-dipole interaction of magnetic nano-particles and the free surface energy of the ball-milled powders could be responsible for the agglomeration of the large particles [17, 19]. The corresponding SAD pattern exhibits diffraction rings for pure cobalt ferrite phase which are completely consistent with its XRD diffraction peaks.

Figure 2 shows the XRD patterns of PEG/CF1 and PVA/CF nano-composites samples. PEG is highly crystalline, having a well-defined crystal structure (Fig. 2a), with strong reflection peaks at 19.23° and 23.35° , and weak reflection peaks at 26.09° , 35.25° and 38.91° , which indicated its crystalline nature, whereas PVA is a semi-crystalline polymer (Fig. 2b) and has a reflection peak at 19.81° and a relatively weak reflection at 40.89° . In PEG/CF1 nano-composite, the crystalline peaks of PEG and cobalt ferrite were observable in both samples, which indicated the presence of PEG in composites. The peaks did not shift by increasing the milling time, but the intensity of PEG peaks has been decreased by 75% during a 10 h milling. Moreover, there was no change in the mean crystallite size of both PEG/CF nano-composites samples did not change drastically (~ 15 nm). However, the interesting result is the obtained nano-composite after 1 h of milling coated and adhered partially to the ball surfaces and the grinding medium. Although this phenomena can be advantageous in some cases since it hinders the wearing of the grinding medium and consequently does not contaminate the products, the thickness of the layer must be a minimum to avoid the formation of heterogeneous product [20]; however, it was in contrasted in this obtained sample in this study, and a great amount of materials covered the balls and vial. In addition, with continued milling for 5 h, the nano-composite powder was transferred to the bulk state in ball mill after cooling down.

Figure 3 (a and b) shows the FESEM and digital camera images of 1 and 5 h milled samples, respectively. This phenomenon can be attributed to the thermal behavior of PEG. PEG has low melting point (Table 1), thus in the initial stage of milling, PEG began to melt due to the local induced heat, and consequently after 5 h the bulk nano-

composite have achieved. Ball-to-wall, ball-to-ball and ball-to-powder collision, and also frictional effects are principal reasons responsible for the temperature rise during milling. According to the literature, more than 90% of the mechanical milling energy given to the powders is transferred to the heat that elevates the temperature of the powders [20].

The nature of the final products is significantly dependent to the induced temperature during milling. Generally, there are two kinds of induced temperature during milling. The first one is the overall temperature in a grinding medium (macroscopic temperature) which varies from 50 to 150°C , though some researchers reported higher temperature rise

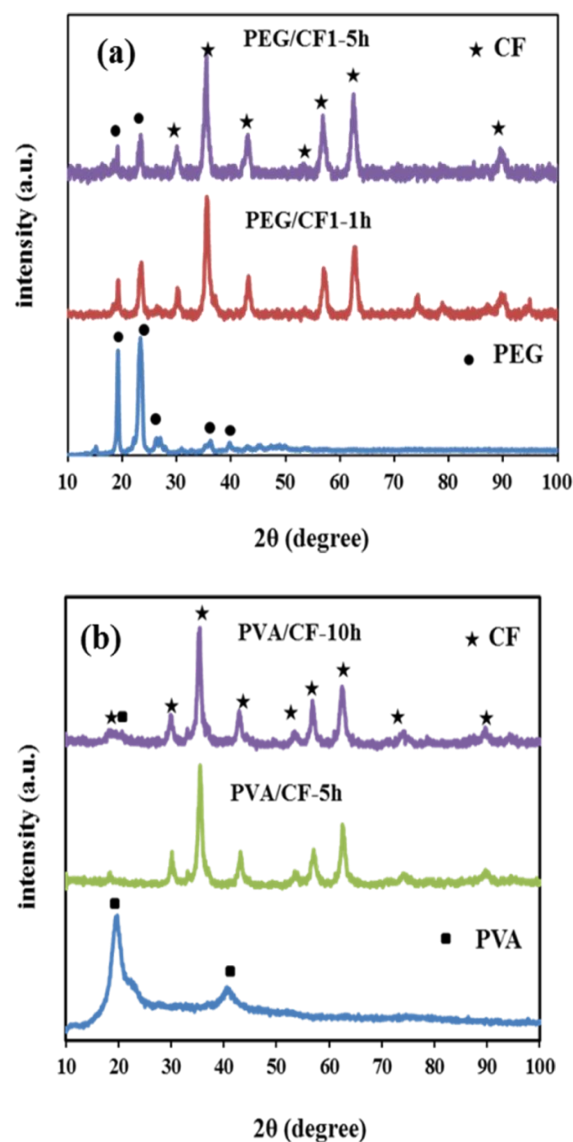


Fig. 2. XRD patterns of (a) PEG/CF1 and (b) PVA/CF nano-composites

(215°C). The other is the local temperature rise due to ball collisions (microscopic temperature). Although this temperature pulses have very short

duration ($\sim 10^{-5}$ s), it can vary very high and often exceeds the melting points of the metals [20, 21].

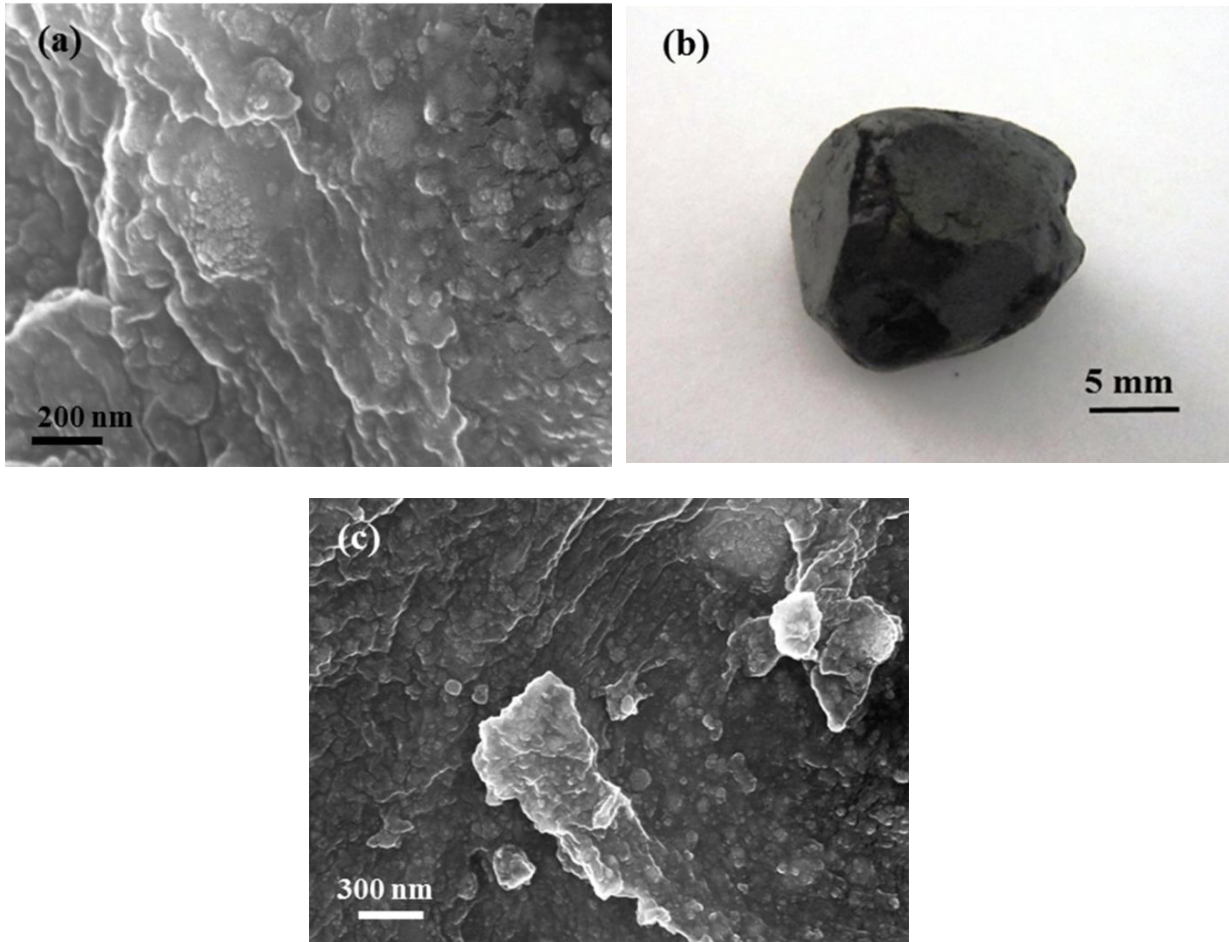


Fig. 3. (a) FESEM image of PEG/CF1 after milling for 5h, (b) digital camera image of PEG/CF1 after milling for 10h and (c) FESEM image of PEG/CF1 after milling for 10 h

As it is seen in Figure 3a the cobalt ferrite particles have been incorporated into the semi-melted PEG matrix, and the amalgamation of the components have been occurred. Due to the obtaining of the bulk result in early stage of milling (5 h), this milling condition collapsed and a more moderate milling condition was chosen for more survey (PEG/CF2 sample). The XRD patterns of this sample after 5 and 10 h of milling (not given here) was entirely similar with PEG/CF1 patterns and no significant changes in the mean crystallite size was observed. It should be said that, in this condition, the PEG was almost completely melted until 10 h of milling as well. FESEM image of PEG/CF2 sample is shown in Figure 3c. Due to the observing similar results, this

sample was not milled for elevated time. Therefore, PEG/CF nano-composites were eliminated from more investigation. It is noteworthy to say that the aim of this work is the preparation of powder nano-composites, so maybe these results could be helpful for preparing samples in bulk amounts.

In XRD patterns (Fig. 2b) of PVA/CF nano-composites, cobalt ferrite preserves its crystalline structure, but the PVA peaks almost disappeared and the intensity of its peak diminished significantly after 5 h of milling time. By further milling, no considerable changes were observed in its intensity. The intensifying reduction of PVA peaks can be reasoned as follows: 1) PVA changes to amorphous state during milling. 2)

PVA decomposes partially to its constituent elements, including C, O and H due to heat and mechanical forces induced during the milling process. The slight shift of cobalt ferrite peaks to higher value can also be justified by the second assumption, by entrancing carbon into cobalt ferrite lattice due to the lower atomic radius of C in comparison with Co^{2+} ionic radius. Furthermore, reduction in milling induced strain ($\Delta d/d$), the term ($\Delta d/d$) is a definition for the concept of strain [22], (from 0.006 to 0.0048; Fig. 4) due to the damping nature of polymer which reduces the milling energy in ball mil can be another reason for changes in peak positions. The crystallite size of cobalt ferrite in PVA/CF sample varies to 13 nm after 10 h of milling (Fig. 4). This variation can be related to the presence of polymer chains which may provide solid surfaces as heterogeneous nuclei for crystallization and the reduced mobility, subsequently prevents the growth of crystals.

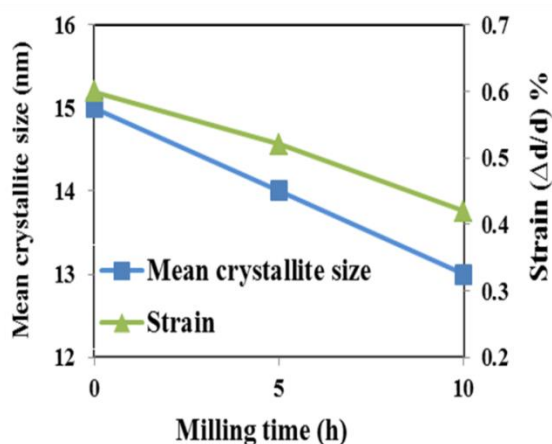


Fig. 4. Mean crystallite size and strain change as a function of milling time in PVA/CF sample (the data of 0 h is related to CF sample)

Presence of cobalt ferrite particles in the polymer matrix classified the mechanical milling process to a ductile-brittle system. Figure 5 shows the possible schematic that illustrates this system. In the first stage of milling, the ductile particles endured deformation, whereas the brittle particles endured fragmentation. Then, when ductile particles began to weld, the brittle particles come into ductile particles at the instant of the ball collisions. As a result, the fragmented reinforcement particles will be embedded in

the interfacial boundaries of the welded powder particles, and a real composite particle was formed. As the welding became the dominant mechanism in the process, the particles changed their morphology. Welding and fracture mechanisms then achieved equilibrium, thus promoting the formation of composite particles with randomly oriented interfacial boundaries. Eventually, at the steady state, the microstructure underwent great refinement [21].

Figure 6 shows the morphology of the PVA/CF nano-composites. As it is seen, the spherical cobalt ferrite nano-particles agglomerates have been dispersed in PVA matrix (Fig. 6a), continuing milling time, up to 10 h, caused the breaking and scattering of cobalt ferrite agglomerates. Also, no melted polymer was observed for PVA/CF nano-composites.

Size of cobalt ferrite nano-particles did not change dramatically (mostly less than 25 nm) after 10 h, as a result of the competition between the fracture and welding phenomena in the milling process. In addition, further milling PVA did not damage and properly milled up to 30 h due to its high melting temperature of PVA. More investigation on this nano-composite will be discussed in our next publication.

FTIR is an appropriate technique to analyze the interaction between polymer chains and magnetic nano-particles. Figure 7 shows the FTIR spectra of pure PVA and PVA/CF nano-composite. The presence of PVA characteristic bands at 3315 cm^{-1} (O-H), 2924 cm^{-1} (C-H), 1710 cm^{-1} (C=O), 1415 cm^{-1} (H-C-H bending), 1132 cm^{-1} (C-O), 1087 cm^{-1} ((M-O-C) M= Co, Fe) and 848 cm^{-1} (CH_2 rocking) in PVA/CF nano-composite confirms the attachment of polymer to the surface of CoFe_2O_4 nano-particles [3, 22]. Moreover, these bands showed a shift to lower wave numbers, which is another clue for interaction. The stretching vibrational bands at 544 cm^{-1} and 465 cm^{-1} were attributed to the intrinsic vibrations of Co-O and Fe-O bonds at the tetrahedral ($\text{M}_{\text{th}}\text{-O}$) and octahedral ($\text{M}_{\text{oh}}\text{-O}$) sites, respectively, for the pure spinel cobalt ferrite which proves the existence of cobalt ferrite in nano-composite [5, 23].

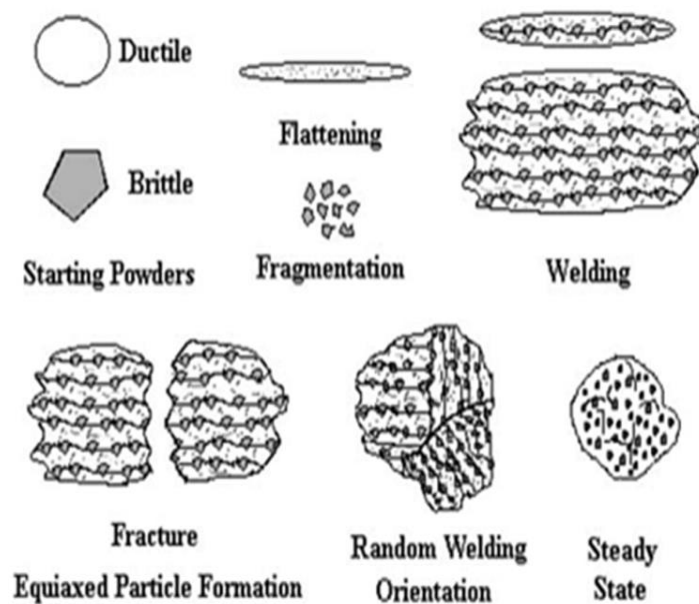


Fig. 5. The different stages of mechanical alloying in ductile-brittle system [21]

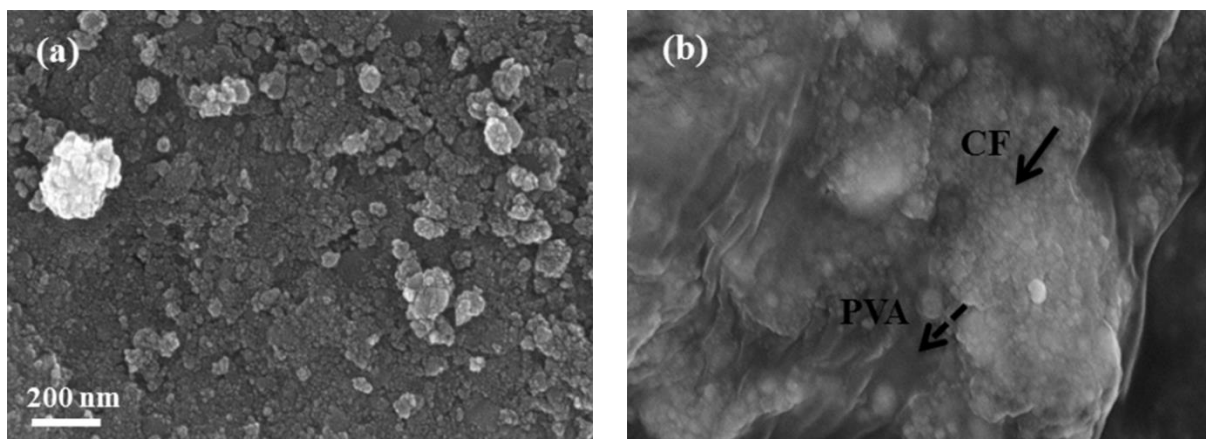


Fig. 6. FESEM images of PVA/CF after milling for (a) 5 h and (b) 10 h

The room temperature M-H loops of cobalt ferrite and PVA/CF samples are shown in Figure 8. The magnetization of the samples under applied field demonstrated clear hysteresis loops referring to their ferromagnetic behavior. The magnetic data are also tabulated in Table 3. It is seen that M_s , M_r , and H_c of nano-composite decreased in comparison with that of pure cobalt ferrite.

The M_s value of PVA/CF sample was approximately proportional to the weight percentage of cobalt ferrite; according to the equation of $M_s = \Phi m_s$, where Φ is the weight fraction of magnetic ferrite particles and m_s is the saturation magnetization of single particles

[24]. The decrease is because of non-magnetic polymer layer on the surface of magnetic nano-particles, which reduces the exchange coupling energy and magnetic particles interactions [3, 25]. Moreover, the coercivity of PVA/CF sample was related to its microstructure. As earlier mentioned above (Fig. 4) the presence of PVA polymer reduced the milling induced strain lattice which causes a reduction in magnetic anisotropy and subsequently nano-composite coercivity [26, 27]. It should be noted that the reduction of particle size also plays a crucial role in decreasing the coercivity in cobalt ferrite [26].

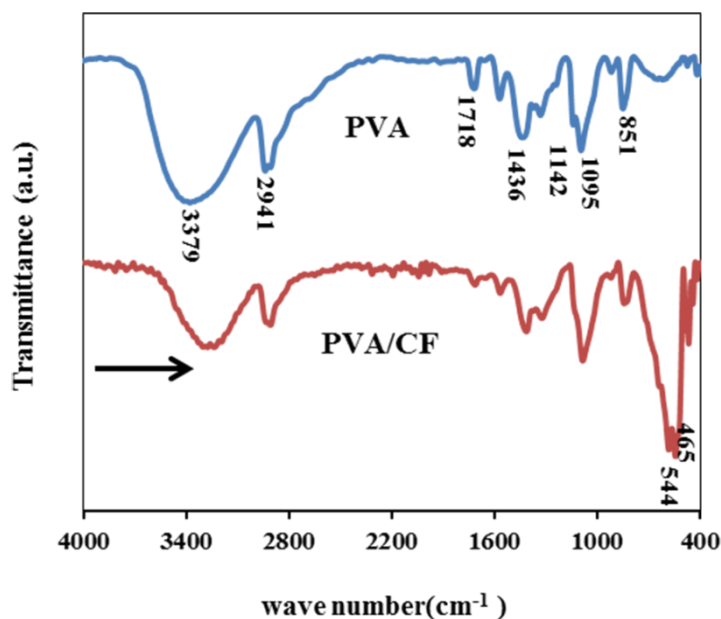


Fig. 7. FTIR analysis of pure PVA and PVA/CF nano-composite

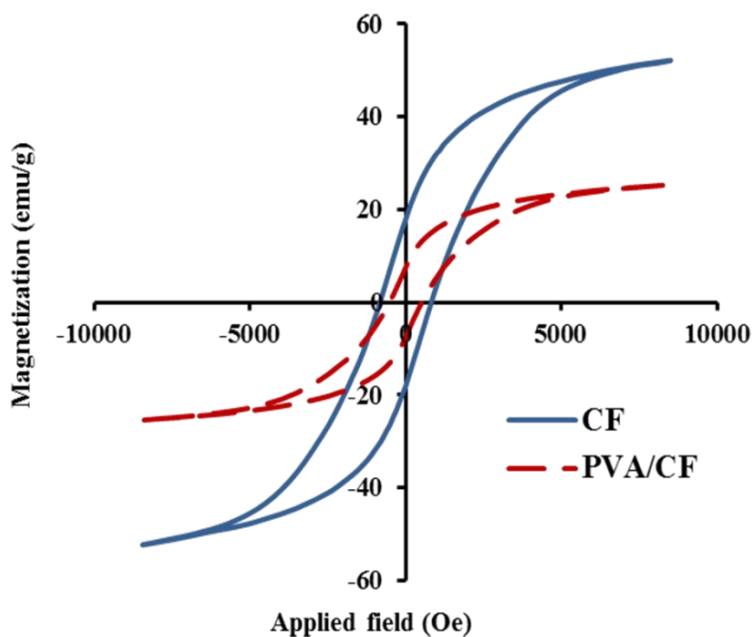


Fig. 8. Hysteresis loops of pure CF and PVA/CF nano-composite

Table 3. Magnetic properties of samples

Samples	M_r (emu/g)	M_s (emu/g)	H_c (Oe)
CF	17.9	52.2	832
PVA/CF	7.4	25.3	519

4. Conclusion

Magnetic nano-composites composed of mixed cobalt ferrite nano-particles and PVA or PEG polymer were synthesized using a two-step mechanical alloying method. PEG could not undergo the local temperature rise and induced heat during milling process, so

melted in both moderate and slow milling conditions. Although, in these nano-composites, cobalt ferrite nano-particles embedded entirely in melted polymer matrix and after the initial hours of milling, the obtained composite changed to bulk in ball mill. PVA was properly mixed with cobalt ferrite particles and the dispersion of particles with interaction between polymer chains and cobalt ferrite nano-particles obtained in the moderate milling condition. This composite had a reasonable magnetic properties ($M_s=25.3$ emu/g and $H_c=519$ Oe) which can be used in various applications, especially in Biomedical field. Accordingly, this method can be versatile for the synthesis of many other polymeric ferrite nano-composites with relatively high thermal resistivity polymer.

Acknowledgements

The financial supports of this work by the University of Tehran and Iran Nanotechnology Initiative Council are gratefully acknowledged.

References

- [1]. Li, S., Lin, M. M., Toprak, M. S., Kim, D. K., Muhammed, M., *Nano. rev.* Vol. 1 (2010) pp. 1-19.
- [2]. Philippova, O., Barabanova, A., Molchanov, V., Khokhlov, A., *Eur. Polym. J.* Vol. 47 (2011) pp. 542-559.
- [3]. Salunkhe, A., Khot, V., Thorat, N., Phadatare, M., Sathish, C., Dhawale, D., Pawar, S., *Appl. Surf. Sci.*, Vol. 264 (2013) pp. 598-604.
- [4]. Qin, R., Li, F., Liu, L., Jiang, W., *J. Alloys Compd.* Vol. 482 (2009) pp. 508-511.
- [5]. Covaliu, C. I., Jitaru, I., Paraschiv, G., Vasile, E., Biriş, S. Ş., Diamandescu, L., Ionita, V., Iovu, H., *Powder Technol.* Vol. 237 (2013) pp. 415-426.
- [6]. Shafiu, S., Topkaya, R., Baykal, A., Toprak, M. S., *Mater. Res. Bull.* Vol. 48 (2013) pp. 4066-4071.
- [7]. Zhang, Q., Zhang, H., Xie, G., Zhang, J., *J. Magn. Mater.* Vol. 311 (2007) pp. 140-144.
- [8]. Huang, J., Pen, H., Xu, Z., Yi, C., *React. Funct. Polym.* Vol. 68 (2008) pp. 332-339.
- [9]. Gorrasi, G., Sorrentino, A., *Green Chem.* Vol. 17 (2015) pp. 2610-2625.
- [10]. Al-Saie, A., Bououdina, M., Jaffar, A., Arekat, S., Melnyczuk, J. M., Thai, Y. T., Brazel, C. S., *J. Alloys Compd.* Vol. 509 (2011) pp. S393-S396.
- [11]. Pan, J., Shaw, W., *J. Appl. Polym. Sci.* Vol. 56 (1995) pp. 557-566.
- [12]. Ishida, T., Tamaru, S., *J. Mater. Sci. Lett.* Vol. 12 (1993) pp. 1851-1853.
- [13]. Zhu, Y., Li, Z., Zhang, D., Tanimoto, T., *J. Appl. Polym. Sci.* Vol. 99 (2006) pp. 501-505.
- [14]. Hedayati, M., Salehi, M., Bagheri, R., Panjepour, M., Maghzian, A., *Powder Technol.* Vol. 207 (2011) pp. 296-303.
- [15]. Raju, P., Murthy, S., *Applied Nanosci.*, Vol. 3 (2013) pp. 469-475.
- [16]. Nathani, H., Gubbala S., Misra, R., *Mater. Sci. Eng., B*, Vol. 111 (2004) pp. 95-100.
- [17]. Rashidi, S., Ataie, A., *Adv. Mater. Res.* Vol. 829 (2014) pp. 747-751.
- [18]. Williamson, G., Hall, W., *Acta Metall.* Vol. 1 (1953) pp. 22-31.
- [19]. Waje, S. B., Hashim, M., Yusoff, W. D. W., Abbas, Z., *Appl. Surf. Sci.* Vol. 256 (2010) pp. 3122-3127.
- [20]. Suryanarayana, C., *Prog. Mater. Sci.* Vol. 46 (2001) pp. 1-184.
- [21]. Abareshi, M., Zebarjad, S. M., Goharshadi, E. K., *J. Vinyl. Additive. Technol.* Vol. 16 (2010) pp. 90-97.
- [22]. Kayal, S., Ramanujan. R., *Mater. Sci. Eng., C*, Vol. 30 (2010) pp. 484-490.
- [23]. Cojocariu, A. M., Soroceanu, M., Hrib, L., Nica, V., Caltun, O. F., *Mater. Chem. Phys.* Vol. 135 (2012) pp. 728-732.
- [24]. Khairy, M., *J. Alloys Compd.* Vol. 608 (2014) pp. 283-291.
- [25]. Reddy, K. R., Lee, K.P., Gopalan, A. I., Kang, H. D., *React. Funct. Polym.* Vol. 67 (2007) pp. 943-954.
- [26]. Singh, S., Munjal, S., Khare, N., *J. Magn. Mater.* Vol. 386 (2015) pp. 69-73.
- [27]. Cedeño-Mattei, Y., Perales-Pérez, O., Uwakweh, O. N., *J. Magn. Mater.* Vol. 341 (2013) pp. 17-24.